Available online at www.sciencedirect.com
SCIENCE DIRECT®
Scripta Materialia 52 (2005) 17–20
Scripta MATERIALIA
www.actamat-journals.com

Structural stability of Ni–Mo compounds from first-principles calculations

Y. Wang [a,*], C. Woodward [b], S.H. Zhou [a], Z.-K. Liu [a], L.-Q. Chen [a]

[a] *Department of Materials Science and Engineering, The Pennsylvania State University, 305 Steidle Building, State College, PA 16802-5006, USA*
[b] *Wright Laboratory ML/MLLM, Wright Patterson AFB, OH 45433-6533*

Received 21 August 2003; received in revised form 10 May 2004; accepted 6 September 2004
Available online 28 September 2004

Abstract

The Ni–Mo alloy system is studied. In contrast to the existing Ni–Mo binary phase diagram that shows three stable compounds, β-Ni_4Mo, γ-Ni_3Mo, and δ-NiMo, it is determined that δ-NiMo is meta-stable at very low temperatures. It is also discovered that two additional compounds, Ni_2Mo and Ni_8Mo are stable at 0 K.

Keywords: Structural stabilities; Ni–Mo binary compounds; δ-NiMo

1. Introduction

Ni-base superalloys have been extensively used for turbine blades in aircraft engines. The continuing demand for higher efficiency engines requires Ni-base superalloys to perform at higher temperatures. One of the key alloying elements in Ni-base superalloys is Mo. In order to understand the effect of Mo content on the microstructure and mechanical properties of Ni-base superalloys, it is important that its effect on phase equilibria be studied starting from the Ni–Mo binary system.

As shown in the Ni–Mo binary phase diagram (see Fig. 1), there exist three known compounds, Ni_4Mo (<870 °C), Ni_3Mo (<910 °C), and δ-NiMo (<1310–1362 °C) [1–4]. They are designated as β-Ni_4Mo ($D1_a$), γ-Ni_3Mo ($D0_a$), and δ-$Ni_{24}[Ni_xMo_{4(5-x)}]Mo_{12}$ ($P2_12_12_1$) (hereafter referred as δ-NiMo). In this work, their stability at 0 K will be studied using total energy first-principles calculations. In addition, we will also examine the stability of other possible ordered intermetallic compounds that are not present in the existing phase diagram. There are experimental evidences that suggest Ni_2Mo and Ni_8Mo might be stable at low temperatures [5,6]. For example, Mayer and Urban [7] reported the observation of ordered Ni_8Mo compound (Ni_8Nb-type structure) [8] and the meta-stable Ni_2Mo compound (Pt_2Mo-type structure). The main objective of this paper is to determine the stability of various compounds in the Ni–Mo binary system. It is expected that findings in this work should lead to significant changes in the intermediate and low temperature part of the existing Ni–Mo phase diagram.

2. Calculation procedure

In this study, we use the Vienna ab initio simulation package (VASP) [9] with the ultrasoft pseudopotentials and the generalized gradient approximation (GGA) [10]. Spin polarized configurations are used for checking the magnetism of the Ni-rich compounds. Energy cutoff is determined by the choice of "high accuracy" in the VASP, i.e., 233.1 eV for Mo and 302.0 eV for Ni and Ni–Mo compounds. For the choice of k points, it is a

* Corresponding author. Tel.: +1 814 8650389; fax: +1 814 8652917.
E-mail address: yuw3@psu.edu (Y. Wang).

1359-6462/$ - see front matter © 2004 Acta Materialia Inc. Published by Elsevier Ltd. All rights reserved.
doi:10.1016/j.scriptamat.2004.09.007

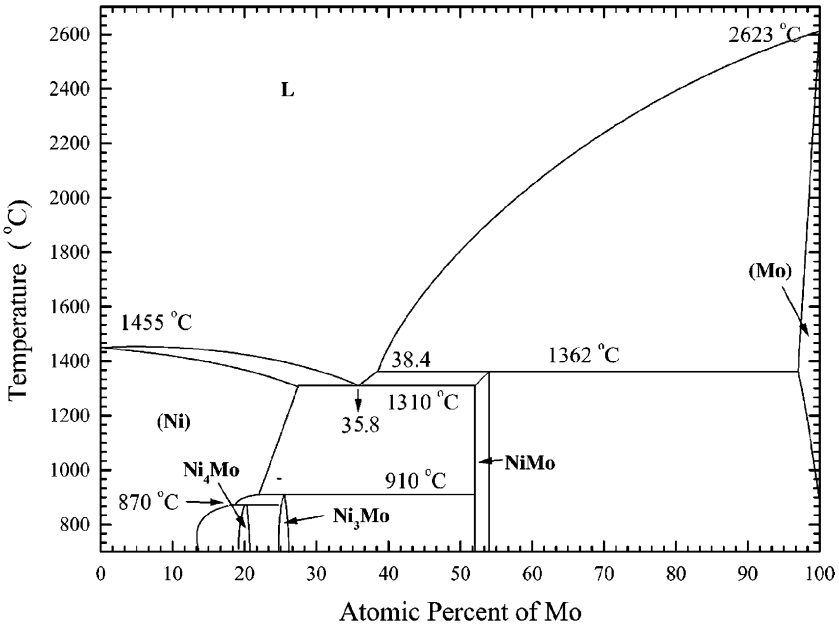

Fig. 1. Ni–Mo alloy phase diagram at high temperature (from Arya et al. [1]).

common practice to keep the product between the number of k points and the number of atoms in the primitive cell being greater than a threshold value (say 3000 or more). In this work, $15\times15\times15$ Monkhost k points for the pure elements, $6\times6\times6$ for δ-NiMo, and $11\times11\times11$ for the other compounds are employed. With the cell shape and the internal atomic coordinates being fully relaxed, the total energies are calculated at seven fixed volume points near the experimental volume, the lowest energy is found by fitting the total energy curve with the Morse function.

In order to perform the total energy calculations, the atomic structures have to be specified first. The primitive cell of δ-Ni_{24} [$Ni_{4x}Mo_{4(5-x)}$]Mo_{12} has 56 atomic sites divided into three types [11]. The first 24 sites are occupied solely by Ni and the last 12 sites are occupied solely by Mo. The 20 sites in the square bracket of the formula δ-Ni_{24}[$Ni_{4x}Mo_{4(5-x)}$]Mo_{12} can be occupied either by Ni or Mo, which are called CN14 sites and assigned as XI, I, III, II, and V by Shoemaker and Shoemaker [11]. Therefore, the various occupation configurations for δ-Ni_{24}[$Ni_{4x}Mo_{4(5-x)}$]Mo_{12} must be considered in the calculation. Due to the limitation on computer resources, we mainly considered the cases where site XI was occupied by Ni since for $x = 1$ the occupation of site XI by Ni was found to give the lowest energy. Thirteen sets of calculations (see Table 1) were performed in the present study for the δ-Ni_{24}[$Ni_{4x}Mo_{4(5-x)}$]Mo_{12} phase.

The structure of Ni_8Mo is body-centered tetragonal [7] built on the face-centered-cubic (fcc) lattice with $a = 3\sqrt{2}/2a_0$, $b = a$, and $c = a_0$ with a_0 being the fcc lattice constant. The structures of other phases can be found in the Pearson's handbook [2], i.e., β-Ni_4Mo has the $D1_a$ structure, γ-Ni_3Mo has the $D0_a$ structure, and Ni_2Mo has the Pt_2Mo structure. The exact atomic positions in the unit cell for $D1_a$, $D0_a$, and Pt_2Mo structures can be downloaded from the Navy Crystal Lattice Structure website [12].

3. Results and discussions

Energy of formation: The energy of formation is obtained as the difference between the total energy of the selected compound and the composition weighted average total energies of the pure elements, namely pure ferromagnetic fcc Ni (−5.4827 eV/atom) and bcc Mo (−10.8271 eV/atom). In the following the energy of formation will be expressed in units of kJ per mole of atoms (kJ/mol). The calculated 0 K energies of formation are listed in Tables 1 and 2 and plotted in Fig. 2.

The energies of formation for Ni_8Mo, Ni_4Mo, Ni_3Mo, and Ni_2Mo from first-principles calculations are listed in Table 2. We found that for Ni_8Mo the magnetic moment is small, 0.03 μ_B/atom, and all the other compounds are non-magnetic. There exist a number of measured values for the enthalpy of formation for the δ-NiMo phase. Spencer and Putland [13] obtained two values for the enthalpy of formation, −1.015 kJ/mol at 973 K and 0.76 kJ/mol at 1573 K. Kubaschewski and Hoster [14] measured another value of 0.21 kJ/mol at 1472 K. A linear extrapolation to 0 K from these three measured data points gives a value of about −4.0 kJ/mol, which is in reasonable agreement with the calculated value of −4.49 kJ/mol in the present work (Table 2). However, for these compounds, our calculated energies of formation are about four times lower than those estimated recently by the thermodynamic modeling of Cui et al. [15].

Table 1
Considered atomic positions for δ-$Ni_{24}[Ni_{4x}Mo_{4(5-x)}]Mo_{12}$ and the corresponding energies of formation

No	Formula	Ni_4 clusters's position[a]	Energy of formation (kJ/mol)
1	$Ni_{24}[Mo_{20}]Mo_{12}$		−3.44
2	$Ni_{24}[Ni_{20}]Mo_{12}$		0.67
3	$Ni_{24}[Ni_4Mo_{16}]Mo_{12}$	XI	−4.49
4	$Ni_{24}[Ni_4Mo_{16}]Mo_{12}$	I	−2.10
5	$Ni_{24}[Ni_4Mo_{16}]Mo_{12}$	XIII	−2.45
6	$Ni_{24}[Ni_4Mo_{16}]Mo_{12}$	II	−1.61
7	$Ni_{24}[Ni_4Mo_{16}]Mo_{12}$	V	−2.14
8	$Ni_{24}[Ni_8Mo_{12}]Mo_{12}$	XI and XIII	−3.44
9	$Ni_{24}[Ni_8Mo_{12}]Mo_{12}$	XI and I	−3.01
10	$Ni_{24}[Ni_8Mo_{12}]Mo_{12}$	XI and II	−2.07
11	$Ni_{24}[Ni_8Mo_{12}]Mo_{12}$	XI and V	−2.20
12	$Ni_{24}[Ni_{12}Mo_8]Mo_{12}$	XI, I, and XIII	−2.19
13	$Ni_{24}[Ni_{16}Mo_4]Mo_{12}$	XI, I, XIII, and II	−1.92

[a] See Shoemaker and Shoemaker [11] for the notation of atomic positions.

Table 2
Energies of formation for Ni_2Mo, Ni_3Mo, Ni_4Mo, and Ni_8Mo

Compound	Ni_2Mo	Ni_3Mo	Ni_4Mo	Ni_8Mo
Energy(kJ/mol)	−8.35	−8.54	−7.55	−4.44

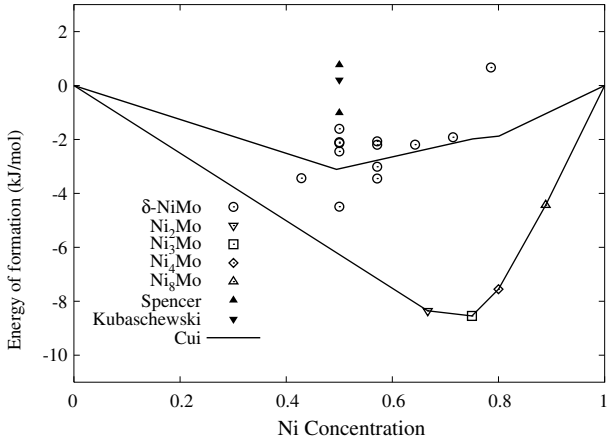

Fig. 2. Energies of formation for various compounds in the Ni–Mo binary system. For the present calculations, ○: δ-NiMo ($P2_12_12_1$ structure); ▽: Ni_2Mo (Pt_2Mo structure); □: γ-Ni_3Mo ($D0_a$ structure); ◇: Ni_4Mo ($D1_a$ structure); △: Ni_8Mo (Ni_8Nb structure). For experiments, ▲: Two points measured at 973 K and 1573 K by Spencer and Putland [13]; ▼: Measured at 1472 K by Kubaschewski and Hoster [14]. The thick solid line shows the modeling result by Cui et al. [15].

The stability of the δ *phase*: For various configurations in the $P2_12_12_1$ structure, our calculations show that $Ni_{24}[Ni_4Mo_{16}]Mo_{12}$ with site XI occupied by Ni has the most negative energy of formation. However, it is metastable with respect to a mixture of its two nearest neighbor phases, Ni_2Mo and pure Mo, at 0 K. The driving force for the decomposition of $Ni_{24}[Ni_4Mo_{16}]Mo_{12}$ into Ni_2Mo and pure Mo is 1.77 kJ/mol at 0 K.

The fact that δ-NiMo is stable at finite temperatures must be from entropic contributions. Entropy can be typically separated into two contributions: the configurational and the vibrational (free energy, more precisely). For the ordered Ni_2Mo and pure Mo, the main entropic contribution can be assumed to be vibrational while for δ-NiMo there is an additional configurational contribution due to the mixing of Ni and Mo in the CN14 sites as reported by Shoemaker and Shoemaker [11].

As an approximation, the vibrational contribution to the free energy can be estimated by calculating the Debye temperatures through bulk modulus as suggested by Slater (see Moruzzi et al. [16] and references therein). Our calculated bulk moduli B for Mo, δ-NiMo, and Ni_2Mo are 255, 235, and 226 GPa, respectively. Wang et al. [17] generalized the model of Slater by defining the Debye temperature as

$$\Theta_D^{\lambda} = \frac{1}{k_B}\left\{\frac{1}{2m}\frac{1}{r^{2\lambda}}\frac{\partial}{\partial r}\left[r^{2\lambda}\frac{\partial E_c(r)}{\partial r}\right]\right\}^{1/2}, \quad (1)$$

where k_B represents Boltzmann's constant, m the averaged atomic mass, r the atomic Wigner–Seitz radii, and $E_c(r)$ the 0 K total energy per atom as a function of r ($4\pi/3r^3 = V$, where V represents the averaged atomic volume). With $\lambda = -1$, 0, or 1, the three well-known expressions for Grüneisen parameters can be derived [17] from Eq. (1). We note that at the 0 K equilibrium volume, $\partial E_c(r)/\partial r = 0$, the Debye temperatures calculated by $\lambda = -1$, 0, and 1 are the same. Our calculated Debye temperatures at 0 K for Mo, δ-NiMo, and Ni_2Mo are 370, 384, and 388 K, respectively. In the case of $\lambda = -1$, Eq. (1) will be reduced to $C(rB/m)^{1/2}$, the one used by Moruzzi et al. [16]. The vibrational free energy can then be expressed in term of Θ_D^{λ} by [16,17]

$$F(V,T) = E_c(r) + \frac{9}{8}k_B\Theta_D^{\lambda}(r) - k_BT\{D[\Theta_D^{\lambda}(r)/T] - 3\ln[1 - e^{\Theta_D^{\lambda}(r)/T}]\}, \quad (2)$$

where $D(x)$ is the Debye function [16,17]. It should be noted that with the increasing temperature, the thermal expansion induced by Eq. (2) makes $\partial E_c(r)/\partial r \neq 0$, which results in small differences for the Debye temperatures by Eq. (1) with respect to different choice of λ. For simplicity, we use $\lambda = 0$ in this work. We found that all three phases have a very similar vibrational free energy change as a function of temperature (different choice of λ does not affect this conclusion).

Assuming an ideal mixing of Ni and Mo in the CN14 sites for δ-NiMo, the configurational entropy of formation for δ-NiMo (ΔS_{mix}) is [18]:

$$\Delta S_{mix} = -R[y\ln y + (1-y)\ln(1-y)], \quad (3)$$

where R is the gas constant, and y the site fraction of Ni on the CN14 sites in δ-NiMo. For $y = 4/20 = 0.2$ with

the lowest energy of formation, the contribution to the Gibbs energy due to the random mixing, $-T\Delta S_{mix}$, would offset the driving force for δ-NiMo to decompose and make δ-NiMo stable at temperatures higher than 426 K.

Structure of the δ phase: The assignment of orthorhombic $P2_12_12_1$ by Shoemaker and Shoemaker [11] several decades ago is commonly accepted [1]. However, the more recent work by Jin et al. [19] suggested a tetragonal P4/mmm structure. In our calculation we started with the $P2_12_12_1$ structure, but relaxed both the shape of the cell and the internal coordinates. We derived $a = 0.9104$ nm, $b = 0.9106$ nm, and $c = 0.8899$ nm. This is in excellent agreement with those given by Shoemaker and Shoemaker, $a = b = 0.9108 \pm 0.0005$ nm and $c = 0.8852 \pm 0.0005$ nm. It should be pointed out that although our calculations indeed show $a \neq b$, the difference is only 0.0002 nm which is well within the experimental uncertainty of 0.0005 nm.

The stability of Ni_3Mo, Ni_4Mo, Ni_2Mo and Ni_8Mo: Ni_3Mo and Ni_4Mo are two of the commonly observed phases in the Ni–Mo high temperature phase diagram. Our first-principles calculations confirm that they are also stable at 0 K. However, for Ni_2Mo and Ni_8Mo, although they are not in the existing phase diagram, they are found to be stable in the first-principles calculations at 0 K, indicating that they are stable at low temperatures. Ni_8Mo has the Ni_8Nb structure while Ni_2Mo has the Pt_2Mo structure. There have been conflicting experimental evidences on the existence of Ni_2Mo at relatively high temperatures. For example, the alloy 76Ni–13Al–9Mo–2Ta aged at 1033 K by Pearson et al. [5] showed evidence for the existence of the compound Ni_2Mo, whereas the experimental determination of the phase equilibrium by Heijwegen et al. [20] indicated that there was no Ni_2Mo phase at 1073 K. There also exists experimental evidence that Ni_8Mo might be stable. For example, Mayer and Urban [7] even provided a critical temperature 555 ± 10 K for its stability through a high-voltage electron microscope observations. Our first-principles calculations thus confirmed that both Ni_2Mo and Ni_8Mo are stable compounds in the Ni–Mo system.

4. Summary

The structural stabilities of five intermetallic phases, i.e., Ni_8Mo, β-Ni_4Mo, γ-Ni_3Mo, Ni_2Mo, and δ-$Ni_{24}[Ni_{4x}Mo_{4(5-x)}]Mo_{12}$ ($0 \leqslant x \leqslant 5$) in the Ni–Mo binary system are studied by calculating their total energies at 0 K using first-principles calculations. It is found that the δ phase is meta-stable at 0 K. It is also found that there should exist additional compounds, Ni_2Mo and Ni_8Mo, in the system. The findings in this work will be incorporated in future thermodynamic modeling of the system and are expected to lead to major changes in the Ni–Mo binary phase diagram.

Acknowledgments

This work is supported by the NASA UEET program under Grant No. NCC3-920. The authors wish to thank Dr. Jorge Sofo for his valuable help and advice. Calculations were carried out on the IBM-SP3 supported by the DOD High Performance Computer Modernization Program at the ASC-MSRC, and the LION-XL cluster at the Pennsylvania State University supported in part by the NSF grants (DMR-0205232, DMR-9983532 and DMR-0122638) and in part by the Materials Simulation Center at the Pennsylvania State University.

References

[1] Arya A, Banerjee S, Das GP, Dasgupta I, Saha-Dasgupta T, Mookerjee A. Acta Mater 2001;49:3575.
[2] Villars PC, Calvert LD. Pearson's handbook of crystallographic data for intermetallic phases. Newbury, OH: ASTM International; 1991.
[3] Arya A, Dey GK, Vasudevan VK, Banerjee S. Acta Mater 2002;50:3301.
[4] Banerjee S. Sadhana 2003;28:799.
[5] Pearson DD, Kear BH, Lemkey FD. In: Wilshire B, Kear Owen DRJ, editors. Factors controlling the creep behavior of a nickel-base superalloy. Swansea: Pineridge; 1981. p. 213.
[6] Ardell AJ. In: Ardell Faulkner JS, Jordan RG, editors. Metallic alloys experimental and theoretical perspectives. Netherlands: Kluwer Academic Publishers; 1994. p. 93.
[7] Mayer J, Urban K. Phys Stat Sol (a) 1985;90:469.
[8] Larson JM, Taggart R, Polonis DH. Metall Trans 1970;1:485.
[9] Kresse G, Demuth T, Mittendorfer F. VAMP/VASP, http://cms.mpi.univie.ac.at/vasp/, 2003.
[10] Perdew JP, Wang Y. Phys Rev B 1992;45:13244.
[11] Shoemaker CB, Shoemaker DP. Acta Cryst 1963;16:997.
[12] http://cst-www.nrl.navy.mil/lattice/index.html, August 21st, 2003.
[13] Spencer PJ, Putland FH. J Chem Thermodyn 1975;7:531.
[14] Kubaschewski O, Hoster T. Z Metallkd 1983;74:607.
[15] Cui Y, Jin Z, Lu X. Metall Mater Trans A 1999;30A:2735.
[16] Moruzzi VL, Janak JF, Schwarz K. Phys Rev B 1988;37:790.
[17] Wang Y, Ahuja R, Johansson B. Int J Quantum Chem 2004;96:501.
[18] Saunders N, Miodownik AP. CALPHAD (Calculation of Phase Diagrams): A Comprehensive Guide. Oxford, New York: Pergamon; 1998.
[19] Jin Y, Han YF, Chaturvedi MC. Mater Lett 1995;23:21.
[20] Heijwegen CP, Rieck GD. Z Metallkd 1973;64:450.